AIAA JOURNAL
Vol. 46, No. 7, July 2008

Calculation of Multidimensional Flames Using Large Chemical Kinetics

Viswanath R. Katta*
Innovative Scientific Solutions, Inc., Dayton, Ohio 45440
and
William M. Roquemore†
U.S. Air Force Research Laboratory, Wright-Patterson Air Force Base, Ohio 45433

DOI: 10.2514/1.33131

A time-dependent, two-dimensional, detailed-chemistry computational fluid dynamics model, known as UNICORN (unsteady ignition and combustion using reactions), is used for solving complex flame problems. The unique features incorporated in UNICORN for handling extremely large chemical kinetics with ease and efficiency are discussed. A submixture concept that is used for evaluating transport properties is described. This concept increases the computational speed by a factor of five for a 208-species mechanism and is expected to have even higher efficiency with larger mechanisms. An implicit treatment for certain reaction-rate terms applied during the solution of species-conservation equations is described. Moving the reaction-rate source terms to the left-hand side of the partial differential equations eases the stiffness problem that is typically associated with combustion chemical kinetics. Computational speeds are further improved in UNICORN by completely integrating the chemical-kinetics mechanisms with the solution algorithm. A software-generated computational fluid dynamics approach is used to avoid the tedious and near-impossible task of manually integrating a large chemical-kinetics mechanism into a computational fluid dynamics code. Several calculations demonstrating the abilities of the UNICORN code are presented. Chemical-kinetics mechanisms up to 366 species and 3700 reaction steps are incorporated, and simulations for unsteady multidimensional flames are performed on personal computers. Making use of the robustness and efficiency of the UNICORN code, detailed chemical mechanisms developed for JP-8 fuel are tested for their accuracy, and a parametric study on the role of parent species of a surrogate mixture in predicting flame extinguishment is performed. Ease of changing chemical kinetics in the UNICORN code is demonstrated through the investigation of effects of additives in JP-8 fuel.

Nomenclature

C_i	=	chemical symbol for the ith species
D_{ij}	=	diffusion coefficient in a binary mixture of the ith and jth species
$D_{i,\mathrm{mix}}$	=	binary-diffusion coefficient of the ith species in a mixture
$f(Y_i)$	=	first variable used in the modified species-conservation equation
$g(Y_i)$	=	second variable used in the modified species-conservation equation
I_i^j	=	availability of the ith species in the reactants of the jth reaction
J_i^j	=	availability of the ith species in the products of the jth reaction
k_j	=	rate of the jth reaction
M_i	=	molecular weight of the ith species
N_s	=	number of species in the chemical kinetics
N_R	=	number of reactions in the chemical kinetics
p	=	pressure
r	=	radial distance
T	=	temperature
t	=	time
u	=	axial velocity component
$\mathbf{V}$	=	velocity
v	=	radial velocity component
X_i	=	mole fraction of the ith species
$X_{\min}$	=	minimum mole fraction in submixture
Y_i	=	mass fraction of the ith species
z	=	axial distance
$\Delta_{f\|T}$	=	flame thickness based on temperature distribution
$\Delta_{f\|\mathrm{OH}}$	=	flame thickness based on hydroxyl-radical distribution.
δ_i	=	error in the ith species in percent
$\partial/\partial t$	=	differential operator with respect to t
η	=	simulation time
η_0	=	simulation time when $X_{\min} = 0$
λ_i, λ_{mix}	=	thermal conductivity of the ith species and mixture, respectively
μ_i, μ_{mix}	=	viscosity of the ith species and mixture, respectively
$\nu'_{i,j}$	=	stoichiometric coefficient for the ith species appearing as reactant in the jth reaction
$\nu''_{i,j}$	=	stoichiometric coefficient for the ith species appearing as product in the jth reaction
ρ	=	density
ϕ, ϕ'	=	functions
χ_{st}	=	scalar dissipation rate at stoichiometry
$\Omega^{(1,1)*}$	=	reduced collision integral
ω	=	production rate
∇	=	Laplace operator

Presented as Paper 4418 at the 37th AIAA Fluid Dynamics Conference and Exhibit, Miami, FL, 25–28 June 2007; received 28 June 2007; revision received 7 March 2008; accepted for publication 17 March 2008.

*Senior Engineer, 2766 Indian Ripple Road; vrkatta@erinet.com. AIAA Associate Fellow.

†Senior Scientist, Propulsion Directorate, Building 5, 1950 Fifth Street; melvyn.roquemore@wpafb.af.mil. AIAA Fellow.

I. Introduction

DETAILED chemical kinetics for describing combustion of aviation fuels involves several hundred species and several thousand elementary reactions. The need for more accurate and presumably larger chemical-kinetics mechanisms is strongly driven by the escalating cost of petroleum-based fuels and the need to

develop alternative and Fischer–Tropsh fuels. Indeed, new fuel mechanisms are being developed at a rapid pace. Traditionally, such newly developed mechanisms are validated through the simulations of zero- and one-dimensional flames using codes such as RUN1DL [1], OPPDIF [2], and CHEMKIN [3] and comparing the results with available experimental data. Extensive experimental data for the intermediate species concentrations are required for obtaining a reasonably calibrated kinetics mechanism. However, in many cases, it is not feasible to obtain concentrations of the numerous hydrocarbon intermediates that are generated during the combustion of complex hydrocarbon fuels such as JP-8. As a result, newly developed, complex chemical-kinetics mechanisms can be only validated partially using traditional approaches.

One of the risks in using partially validated mechanisms is that the simulations for a reacting flow under one set of conditions may appear to be reasonable, whereas under a different set of conditions they may be poor. This was demonstrated by Katta et al. [4] using recently developed mechanisms for JP-8 fuels. Three JP-8 mechanisms were investigated: one from Ranzi's group at Politeccnico di Milano, the second from the University of Utah, and the third from the Propulsion Directorate of the Air Force Research Laboratory (AFRL/RZ). These mechanisms were developed independently and validated using the limited experimental data on ignition delay times and flame speeds. The Violi mechanism (Ranzi's group) [5] has 161 species and 1538 reactions, including some global-type reactions; the University of Utah mechanism [6] has 208 species and 2186 reactions, and the Mawid Mechanism (AFRL/RZ) [7] has 216 species and 3000 reactions. These three mechanisms were incorporated in UNICORN [8] (unsteady ignition and combustion using reactions), and calculations were performed for a variety of two-dimensional flame systems. It was found that the flame structures predicted by these mechanisms were radically different and, more important, that the blowout characteristics of a nonpremixed flame varied significantly from mechanism to mechanism. Disappointingly, the partially validated chemistry models were found to be of only limited use in the simulation of multidimensional flames.

Thus, a second-level validation must be performed on partially validated chemistry models through the simulation of two- or three-dimensional flames and by comparing the global features such as flame shape, size, and liftoff height. As these global quantities can easily be measured in the laboratory, a second-level validation for the detailed-chemistry models can be performed if computational fluid dynamics (CFD) codes that can incorporate large-chemical-kinetics mechanisms and perform simulations for multidimensional flames are available.

Advances in computer hardware technology and the need to improve the understanding of combustion phenomena such as flame stability, pollutant formation, and lean blowout have led to the development of CFD codes with detailed chemical kinetics [9–11]. However, due to the fact that computational time increases significantly with the size of the chemical-kinetics mechanism used, CFD code developments are limited to either simple fuels, such as hydrogen [12], methane [13], and ethylene [14], that are described with smaller detailed mechanisms (less than 100 species) or to complex fuels such as propane [15], heptane [16], and JP-8 [17] that are described with reduced mechanisms (tens of species).

A two-dimensional numerical model known as UNICORN [8], which has the capability to incorporate detailed chemical-kinetics mechanisms, has been developed at AFRL/RZ for the simulation of dynamic, nonpremixed, and premixed jet flames. This model is being used for studying flame systems and evaluating large chemical mechanisms and soot models on programs sponsored by the U.S. Air Force Office of Scientific Research and the Strategic Environmental Research and Development Program.

The present paper describes extension of the UNICORN code to incorporate very large chemical-kinetics mechanisms and to simulate multidimensional flames efficiently and accurately. Various simulations that were performed for demonstrating the capabilities of the modified UNICORN code are discussed.

II. Mathematical Model

The UNICORN code [8,18] is a time-dependent, axisymmetric mathematical model that is used for the simulation of unsteady reacting flows. It is capable of performing direct numerical simulations and has been developed over a 10-year period. Its evolution has been in conjunction with experiments conducted to test its ability to predict ignition, extinction, stability limits, and the dynamic characteristics of nonpremixed and premixed flames of various fuels. It solves for u- and v-momentum equations, and continuity, and enthalpy- and species-conservation equations on a staggered-grid system. The body-force term due to the gravitational field is included in the axial-momentum equation for simulating vertically mounted flames. A clustered mesh system is employed to trace the large gradients in flow variables near the flame surface. Detailed chemical-kinetics models for various fuels are incorporated. Thermophysical properties such as enthalpy, viscosity, thermal conductivity, and binary molecular diffusion of all of the species are calculated from the polynomial curve fits developed for the temperature range 300–5000 K. Mixture viscosity and thermal conductivity are then estimated using the Wilke [19] and Kee [20] expressions, respectively. Molecular diffusion is assumed to be of the binary-diffusion type, and the diffusion velocity of a species is calculated using Fick's law and the effective-diffusion coefficient of that species [21] in the mixture. A simple radiation model based on the optically thin-media assumption is incorporated into the energy equation.

The finite-difference forms of the momentum equations are obtained using an implicit QUICKEST (quadratic upstream interpolation for convective kinematics with estimated streaming terms) scheme [18,22], which is fourth-order accurate in space and third-order accurate in time. The species and energy equations are descretized using a hybrid scheme of upwind and central differencing, which is second-order accurate in both time and space. At every time step, the pressure field is accurately calculated by solving all of the pressure Poisson equations simultaneously and using the lower and upper diagonal matrix-decomposition technique. The overall accuracy of the calculations made by the UNICORN code is estimated to be second-order or better in both time and space. As demonstrated in the past [23], it is possible to simulate two-dimensional turbulent flows (where no significant variation in flow variables exists in the third dimension) using UNICORN. However, for brevity, the scope of the present paper is limited to steady and unsteady laminar flames. Different types of boundary conditions such as adiabatic wall, isothermal wall, symmetric surface, outflow, and inflow can be applied to the boundaries of the computational domain [24].

III. Computational Procedure

In theory, the mathematical model described previously is sufficient for the simulation of multidimensional flames using large chemical kinetics. However, because of limitations on computational resources and difficulties associated with incorporating chemical-kinetics models, to obtain a multidimensional-flame solution using a large chemical-kinetics mechanism within a reasonable amount of time is a daunting task. Four computational techniques have been incorporated in UNICORN to make it efficient and robust in simulating multidimensional flames on personal computers.

A. Nonuniform Grid System

The accuracy of a simulation performed using a finite-difference scheme depends on the grid resolution. Typically, one obtains a grid-independent solution by performing calculations on increasingly finer meshes until the solution attains quasi-steady state (mesh independent). The finite-difference forms of the governing equations in the UNICORN code are obtained on a nonuniform, orthogonal mesh system and are solved using semi-implicit procedures [18]. These procedures, due to fewer restrictions on the time step, allow the use of rapidly expanding grid sizes in both the axial and the radial directions. Because the reaction-zone of a flame is confined to a

narrow region within the high-temperature zone, grid distribution must be sufficiently fine in that region. Variable grid systems are constructed a priori while enforcing clustering of grid points in the neighborhoods of the reaction zones, while allowing the grid spacing to expand rapidly as the grid points are located away from these regions. This facilitates the use of a minimum number of grid points for the simulation of a given flame. Calculations are made first on a coarse-grid system and then on a fine-mesh system, using the previously obtained solution as the initial conditions. The implicit procedures used in the UNICORN code permit stable calculations, even when large variations in grid spacing are present between the coarse- and fine-mesh systems. Overall, fewer grid points and systematic progress toward a fine-mesh solution allow the UNICORN code to perform multidimensional simulations with large chemical kinetics efficiently.

B. Calculation of Transport Properties

As described previously, the transport properties for the mixture are calculated using Wilke's [19] and Kee's [20] empirical expressions. Mixture thermal conductivity λ_{mix} and viscosity μ_{mix} can be calculated as follows for a mixture with N_s species:

$$\lambda_{\text{mix}} = \sum_{i=1}^{N_s} \lambda_i \left[1 + \frac{1.065}{2\sqrt{2} X_i} \sum_{k \neq i}^{N_s} X_k \phi_{ik} \right]^{-1} \quad \text{with}$$
$$\phi_{ik} = \frac{[1 + (\lambda_i^0/\lambda_k^0)^{1/2} (M_i/M_k)^{1/4}]^2}{[1 + M_i/M_k]^{1/2}} \tag{1}$$

$$\mu_{\text{mix}} = \sum_{i=1}^{N_s} \mu_i \left[1 + \frac{\sqrt{2}}{4X_i} \sum_{k \neq i}^{N_s} X_k \phi'_{ik} \right]^{-1} \quad \text{with}$$
$$\phi'_{ik} = \frac{[1 + (\mu_i/\mu_k)^{1/2} (M_i/M_k)^{1/4}]^2}{[1 + M_i/M_k]^{1/2}} \tag{2}$$

Here, λ_i and μ_i are thermal conductivity and viscosity of the individual species, respectively, and M_i and X_i are species molecular weight and concentration, respectively. Similarly, the effective-diffusion coefficient of the ith species in a mixture [21] is calculated using the empirical expression

$$D_{i,\text{mix}} = \frac{1 - X_i}{\sum_{i \neq j}^{N_s} X_j / D_{ij}} \quad \text{with}$$
$$D_{ij} = \frac{2.628 \cdot 10^{-3}}{p \rho^2 \Omega_{i,j}^{(1,1)*}} \left[\frac{T^3 (M_i + M_j)}{2 M_i M_j} \right]^{1/2} \tag{3}$$

D_{ij} is the binary-diffusion coefficient between species i and j, and $\Omega_{i,j}^{(1,1)*}$ is the reduced collision integral. Calculation of the mixture transport properties for systems with a large number of species is laborious and requires far more computational time than that required for solving the conservation equations or the reaction rates. Examination of Eqs. (1) and (2) suggests that, in a system having N_s species, ϕ and ϕ' must be evaluated (N_s^2-N_s) number of times at each grid point. For example, in a system of 300 chemical species, ϕ and ϕ' must be evaluated 89,700 times each, which is nearly 18 times more than the number of calculations required for evaluating reaction rates for 5000 reactions. As N_s increases, evaluation of λ_{mix} and μ_{mix} becomes increasingly time consuming. However, in multidimensional-flame calculations, most of the species will be present in trace amounts in regions away from the flame zone and only in parts per million levels in the flame zone. Because trace concentrations of species do not affect the thermal conductivity or viscosity of the mixture, it is possible to increase the speed of the calculations by considering only those species that are in significant concentrations. This can be accomplished by creating a submixture at every grid point through elimination of all species that are below a specified concentration in the entire mixture and then evaluation of transport properties using only the submixture. Note that diffusion coefficients $D_{i,\text{mix}}$ are evaluated by using Eq. (3) and considering all of the species in the mixture, because the benefit of using the submixture in this case is minimal.

In the simulation of a two-dimensional nonpremixed jet flame, increasing the speed of the calculations through use of the submixture concept is demonstrated in Fig. 1. A 208-species, 1093-reaction, chemical-kinetics model for JP-8 fuel is used for this demonstration. Calculations for the flame are repeated by changing the minimum concentration allowed in the submixture. The computational time for each simulation is normalized with that required by the original simulation that considered all of the species while evaluating the transport properties. The minimum concentration allowed in the submixture is shown in log scale on the horizontal axis. For each simulation percentage error, δ_i is obtained first by calculating the difference in the concentration of the ith species predicted with the submixture concept and that of the original simulation and then by normalizing this difference to the original value. Errors estimated based on the peak H radical and byphenyl poly-aromatic-hydrocarbon concentrations at a flame height of 4 cm are shown in Fig. 1. Note that errors in the concentrations of major species, temperature, and velocity are negligible.

A dramatic reduction in calculation time (by a factor of five) is achieved by considering species whose concentrations are $>10.0^{-03}$ for transport-property evaluation purposes, whereas the errors introduced are <1% in minor- and trace-species concentrations. It is important to note that the reduction shown in Fig. 1 is for the entire flame simulation (not just for the transport-property calculation) which gives some indication of the large percentage of computational time required for calculating mixture transport properties alone. Because the increase in speed of calculation is proportional to the square of the number of species, the benefit of using submixtures becomes more pronounced as the number of species in the chemical-kinetics model increases.

C. Handling Stiff Equations

Species-conservation equations can be written as following using Fick's law of diffusion for binary mixtures and the effective-diffusion coefficient $D_{i,\text{mix}}$ for the ith species in the mixture.

$$\frac{\partial \rho Y_i}{\partial t} + \nabla \cdot [\rho Y_i \mathbf{V} - \rho D_{i,\text{mix}} \nabla Y_i] = \dot{\omega}_i \tag{4}$$

Here, the source term $\dot{\omega}_i$ is the rate of production of the ith species that must be calculated from the adopted chemical-kinetics mechanism, which is written in the following form:

$$\sum_{i=1}^{N_s} \nu'_{i,j} C_i \xrightarrow{k_j} \sum_{i=1}^{N_s} \nu''_{i,j} C_i \qquad j = 1, N_R \tag{5}$$

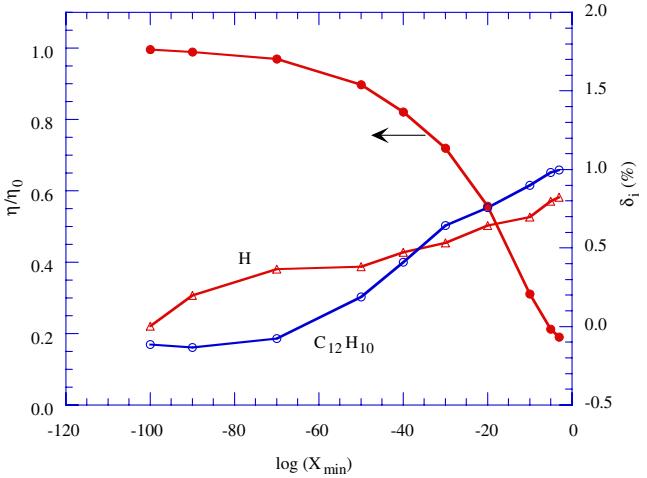

Fig. 1 Computational time required and associated errors for different minimum concentrations allowed in submixture domain.

Here, C_i represents chemical symbol for the ith species and N_R represents the total number of reactions in the chemical-kinetics mechanism. Note that all reactions in the mechanism are written as forward reactions.

In general, because of the high reaction rates (and, hence, large $\dot{\omega}_i$ values) associated with the combustion processes, species-conservation equations become very stiff; traditionally, small time steps are used in solving Eq. (4) to overcome this stiffness problem. However, such an approach places severe restrictions on multidimensional-flame simulations because the flow time scales associated with certain domains such as recirculation and coflow-entrainment regions are several orders of magnitude larger than the chemical time scales. Therefore, special techniques are required for solving Eq. (4) with larger time steps in multidimensional-flame simulations. After expanding the source terms into destruction and production terms, Eq. (4) can be rewritten as

$$\frac{\partial \rho Y_i}{\partial t} + \nabla \cdot [\rho Y_i \mathbf{V} - \rho D_{i,\mathrm{mix}} \nabla Y_i] = -\sum_{j=1}^{N_R} (\nu'_{i,j} - \nu''_{i,j}) k_j \prod_{m=1}^{N_s} \left(\frac{Y_i}{M_i}\right)^{\nu'_{m,j}} \tag{6}$$

and then as

$$\frac{\partial \rho Y_i}{\partial t} + \nabla \cdot [\rho Y_i \mathbf{V} - \rho D_{i,\mathrm{mix}} \nabla Y_i] = -\sum_{j=1}^{N_R} (\nu'_{i,j} - \nu''_{i,j}) k_j I_i^j \left(\frac{Y_i}{M_i}\right)^{\nu'_{i,j}} \prod_{\substack{m=1 \\ m \neq 1}}^{N_s} \left(\frac{Y_i}{M_i}\right)^{\nu'_{m,j}} - \sum_{j=1}^{N_R} (\nu'_{i,j} - \nu''_{i,j}) k_j J_i^j \prod_{m=1}^{N_s} \left(\frac{Y_i}{M_i}\right)^{\nu'_{m,j}} \tag{7}$$

where $I_i^j = 1$ if the ith species is a reactant in the jth reaction, otherwise $I_i^j = 0$, and where $J_i^j = 1$ if the ith species is a product in the jth reaction, otherwise $J_i^j = 0$.

Because the mass fraction of the ith species explicitly appears in the destruction terms (first set of terms on the right-hand side) of Eq. (7), they can be shifted to the left-hand side of the equation for treating them implicitly. Species-conservation equations are then rewritten, after linearizing the destruction terms with respect to Y_i, as

$$\frac{\partial \rho Y_i}{\partial t} + \nabla \cdot [\rho Y_i \mathbf{V} - \rho D_{i,\mathrm{mix}} \nabla Y_i] + \sum_{j=1}^{N_R} (\nu'_{i,j} - \nu''_{i,j}) k_j I_i^j \left(\frac{Y_i}{M_i}\right) \left(\frac{Y_i}{M_i}\right)^{(\nu'_{i,j}-1)} \prod_{\substack{m=1 \\ m \neq 1}}^{N_s} \left(\frac{Y_i}{M_i}\right)^{\nu'_{m,j}} = -\sum_{j=1}^{N_R} (\nu'_{i,j} - \nu''_{i,j}) k_j J_i^j \prod_{m=1}^{N_s} \left(\frac{Y_i}{M_i}\right)^{\nu'_{m,j}} \tag{8}$$

which then takes the following implicit form in terms of Y_i:

$$\frac{\partial \rho Y_i}{\partial t} + \nabla \cdot [\rho Y_i \mathbf{V} - \rho D_{i,\mathrm{mix}} \nabla Y_i] + f(Y_i) \cdot Y_i = g(Y_i) \tag{9}$$

Here, $f(Y_i)$ and $g(Y_i)$ are functions of chemical-kinetics parameters and species mass fractions. Values of these functions are calculated from the data available after the previous time step's solution.

Special care must be taken when the ith species appears in both the reactants and the products of a reaction. Implicit treatment of the destruction terms significantly enhances the stability of the numerical scheme [25] and allows time steps much larger than those allowed by Eq. (9). However, because $f(Y_i)$ and $g(Y_i)$ in Eq. (9) are temporarily treated as constants based on the previous time step's data, the solution procedure previously described for the species-conservation equations represents a semi-implicit algorithm. Note, a fully implicit algorithm can be derived by constructing Jacobian matrices for all of the species involved in the production and destruction terms in Eq. (6), but such procedures become memory and computational-time intensive and may become restrictive in performing multidimensional-flame simulations [26]. Because the primary goal for the development of the UNICORN code is to simulate multidimensional flames using large chemical-kinetics mechanisms, memory-intensive fully implicit algorithms were not used.

D. Incorporating Large Chemical Kinetics

Detailed chemical-kinetics for describing combustion of aviation fuels could involve hundreds of species and thousands of reactions. Such large mechanisms can be used for performing multidimensional reacting-flow simulations by either calculating the reaction rates $\dot{\omega}_i$ in Eq. (4) at each grid point, through calling a mechanism subroutine (such as CHEMKIN) [27] or integrating the mechanism with a CFD code [28,29]. Because the former approach does not require any manipulation of the chemical-kinetics mechanism that has been supplied in a standard format (for example, CHEMKIN format [3]), it eliminates any possible errors in using the chemical-kinetics mechanism for a multidimensional-flame simulation. However, such a calling-mechanism approach puts a significant burden on computational resources. Also, it may become an impractical approach for even a moderately large mechanism, mainly due to the fact that general-purpose codes such as CHEMKIN perform a number of overhead calculations each time they are called. Furthermore, the calling-mechanism approach requires the chemical source terms to be treated explicitly, as in Eq. (4), which is known for its limitations in handling stiff reactions.

Incorporating large chemical-kinetics mechanisms in a CFD code, either through Eq. (4) or Eq. (9), is a formidable task and highly susceptible to typographical and programming errors. Moreover, the implicit treatment of the reaction-rate terms in Eq. (9) and the need for continuous evaluation of functions $f(Y_i)$ and $g(Y_i)$ (as and when new information about a species is available) to ensure a stable-solution procedure make the large chemical-kinetics mechanism incorporation extremely difficult. Because of these difficulties, scientists/engineers rarely use large mechanisms for performing multidimensional reacting-flow simulations. As described in the previous subsection, the UNICORN code was developed based on an implicit algorithm for chemical reactions, and the reaction mechanism must be integrated with the code.

UNICORN uses an innovative approach to achieve efficient calculations for reacting flows with large chemical-kinetics mechanisms. This approach involves the development of a logic program that "reads" a chemical mechanism of any size into UNICORN and automatically configures it in such a way that the calculations run efficiently. To understand this approach, one must realize that UNICORN is optimized for each kinetic mechanism to ensure that reacting flows using the mechanism can be computed efficiently and accurately. Some background is required to understand, in general, how this is accomplished. The UNICORN code is developed based on an implicit algorithm for chemical reactions, which requires that the reaction mechanisms be integrated with the code. During the early development stages of UNICORN, small chemical mechanisms for fuels such as hydrogen and methane were incorporated manually: a very cumbersome and time-consuming task. For example, the total time required for incorporating a 21-species, 81-reaction mechanism into UNICORN was about a month, including the time for debugging and finding and correcting typographical and programming errors. Such developmental time was expected to increase to several months for medium-size mechanisms with less than 100 species. This seemed to be an impractical approach for large mechanisms with more than 200 species. To circumvent this problem, a special logic program has been written that directly reads the chemical-kinetics data that are prepared and distributed in standard CHEMKIN format and writes an efficient, robust version of the UNICORN code for that chemistry. With this approach, a UNICORN code that is optimized for a specific chemical-kinetics model can be developed in a few hours, independent of its size.

The logic program that generates a new UNICORN code in FORTRAN language for the given chemical-kinetics model directly reads the kinetics data prepared in standard CHEMKIN format. This logic program has been rigorously tested on smaller mechanisms to ensure that it generates an error-free UNICORN code for the given chemistry. In this way, human involvement in preparing the CFD code is minimized; hence, errors associated with it are eliminated. Using this software-generated CFD strategy (i.e., accurate development of a modified UNICORN code), a number of reacting-flow simulations have been performed. These include 1) ethylene flames with 99 species and 1066 reactions [30], 2) propane flames with 105 species and 1200 reactions [31], 3) methane + halon flames with 92 species and 1644 reactions [32], and 4) heptane flames with 366 species and 3698 reactions [33].

IV. Results and Discussion

Multidimensional-flame simulations using UNICORN can be performed on a personal computer with 2.0 GB of memory. Execution times depend strongly on the number of species considered in the chemical-kinetics model and the grid size. The ease of use and efficiency of the UNICORN code in handling stiff and large chemical kinetics are demonstrated in the following subsections.

A. Studies on Flame Thickness

The opposing-jet flame shown in Fig. 2 is formed between hydrogen and air jets and represents a weakly stretched laminar flame. The fuel and air jet velocities used are 0.4 and 0.3 m/s, respectively. A 13-species, 74-reaction H_2-O_2-N_2 chemical-kinetics model is used for simulating this flame. As the velocities of the fuel and air jets increase, the flame becomes thinner and its temperature decreases. The flame extinguishes for a critical set of velocities (or strain rates or scalar dissipation rates). Two theories are used to describe the flame-extinction process. According to laminar-flamelet theory [34], the reaction layer of a flame becomes infinitely thin before the flame is extinguished. On the other hand, the distributed-reaction-zone theory of Bilger [35] suggests that the reaction layers are broadened because of chemical equilibrium and that flames cannot be stretched to infinitely thin surfaces. Let us consider the opposing-jet flame shown in Fig. 2 for understanding the flame-extinction process and, particularly, the limits, if any, for flame thickness.

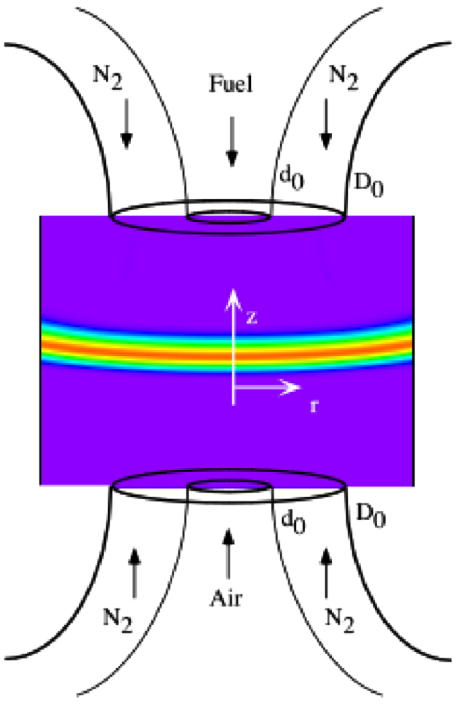

Fig. 2 Opposing-jet nonpremixed flame subjected to strain rates up to extinction limit.

Numerical experiments are performed through increasing the reaction rates in an attempt to approach asymptotically infinitely thin reaction zones. Increasing the reaction rates renders the species-conservation equations stiffer and challenges the numerical algorithm in handling stiff equations. Four sets of data with modified reaction rates are shown in Fig. 3. The results of flame-thickness estimates based on the full width of the temperature profile at various scalar dissipation rates χ_{st} are shown in Fig. 3. Thicknesses of the flame at the time of extinction are marked with open circles. Flame thicknesses obtained after reducing the rates of the 37 forward reactions by one-half are shown with dash-dot lines, whereas that obtained after doubling the rates of the forward reactions is shown with a broken line. Note that increasing or decreasing the forward reaction rates alone (without changing the reverse reaction rates) in a chemical-kinetics mechanism could alter the equilibrium characteristics of the chemical system; hence, such studies should be strictly limited to evaluating the stability of the numerical scheme. Results obtained after doubling the rates of the forward and reverse reactions are shown with thin lines, and those obtained after increasing the rates of both the forward and reverse reactions by an order of magnitude are shown with dotted lines. Changes in reaction rates affect not only the maximum scalar dissipation rate (or stretch rate) that can be applied on this flame, but also the temperature at which extinction takes place. In general, temperature and heat release rates at extinction are higher with faster reactions. At a given scalar dissipation rate χ_{st}, the temperature and heat release rate of the flame increases with the reactivity of the system. The increase is more pronounced at higher χ_{st}. This behavior can be explained considering the chemical-nonequilibrium state of the flame. An increase in the reaction rates enhances the reactivity in the flame zone and, thereby, shifts the flame more into equilibrium.

Figure 3 suggests that the thickness of the steady opposed-jet flame decreases, as described by the laminar-flamelet theory, when the stretch rate is increased. However, contrary to the assumption that stretched flames become infinitely thin before extinction, flame thicknesses at extinction obtained with normal, reduced, and enhanced kinetics are all within the range of 1 and 2 mm. More interestingly, the thickness vs χ_{st} plot suggests that flame thickness is asymptotically approaching a finite value ($\sim$1 mm).

One could argue that the temperature profile might not necessarily represent the reaction-zone thickness because it is influenced by the thermal and molecular diffusive transports. Typically, intermediate radical species such as OH, O, and H that have a short life span are confined to reaction zones. Variations of flame thicknesses obtained from the full width of OH radical distributions are shown in Fig. 4. For a given scalar dissipation rate, reaction-zone thicknesses obtained from OH radical distributions are about one-half of those

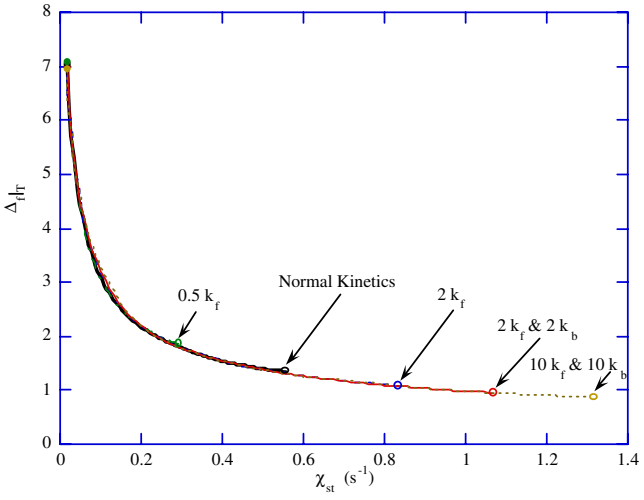

Fig. 3 Thickness of steady-state flame at different stretch rates obtained from temperature.

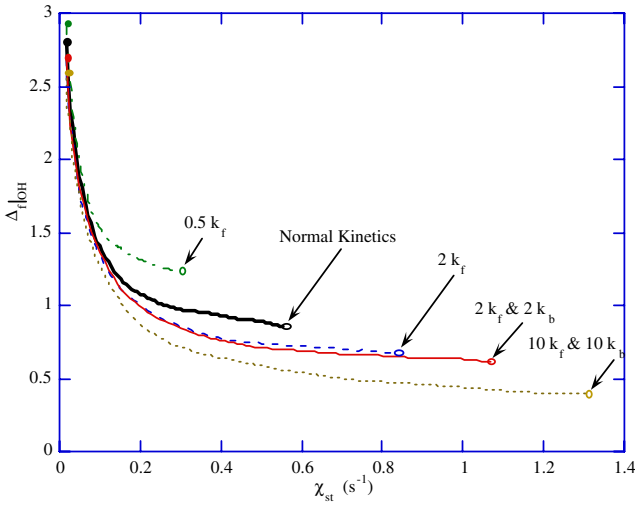

Fig. 4 Thickness of steady-state flame at different stretch rates obtained from OH concentration.

obtained from temperature. Figure 4 suggests that the radical-based reaction-zone thicknesses are also asymptotically approaching a finite value as the scalar dissipation rate on the flame is increased. It is important to note that even the smallest thickness of 0.5 mm represents a radical profile that has been resolved with a large number (25) of grid points; hence, the asymptotic thicknesses shown in Figs. 3 and 4 are not limited by the grid distribution.

Calculations made with different reaction rates suggest that a minimum thickness exists for the reaction zone of a flame that is aerodynamically stretched. For the hydrogen flame considered in this study, the minimum reaction-zone thickness is in the range 0.5–1.0 mm, depending on the radical species used for obtaining the thickness. A similar study of methane flames also suggested that the minimum reaction-zone thickness (based on OH distribution) for those flames is also ∼0.5 mm.

B. Studies on Ethylene–Air Jet Nonpremixed Flames

Calculations for an inverse diffusion flame (IDF) were made with UNICORN using three chemical-kinetics models for ethylene–air combustion. The first model is proposed by Wang and Frenklach [36] and consists of 99 species and 1066 elementary-reaction steps; the second is developed by the National Institute of Standards and Technology (NIST) and consists of 225 species and 1634 elementary reactions [37]; the third is a more comprehensive mechanism assembled by NIST and consists of 366 species and 3698 reactions [37]. Note that all of these mechanisms for ethylene–air combustion are well validated for high-temperature chemical processes, and one should expect similar flame shapes and temperature and major-product-concentration distributions. Larger mechanisms contain additional chemical kinetics required for predicting pollutant formation. The simulated IDF burner consists of a 1-cm-diam central air jet and a 3-cm-diam coannular fuel jet [31,38]. The air and ethylene flow velocities are 35 cm/s and 7 cm/s, respectively. Axisymmetric calculations were made on a physical domain of 200×50 mm using a 401×121 nonuniform grid system. The steady-state flames obtained with the three mechanisms are shown in the left halves of Figs. 5a–5c in plots of isotemperature gray-scale distributions. The three mechanisms predicted the same flame height and peak temperature (2440 K). Typical execution times for these calculations are 30 s/time step with the Wang–Frenklach mechanism, 65 s/time step with the NIST smaller mechanism, and 114 s/time step with the NIST larger mechanism. Steady-state flames were obtained in about 2000 time steps, starting from the solution obtained with a global-chemistry UNICORN code.

Various studies of normal jet nonpremixed flames (i.e., with the fuel jet at the center) suggest that when the annular airflow is low (<40 cm/s), the flame tends to flicker with the development of buoyancy-induced vortices outside the flame surface. Generally, the flickering frequency for these flames is independent of or weakly dependent on fuel-jet diameter, fuel type, and airflow velocity. The low annular fuel velocity of ∼7 cm/s and the high-enthalpy ethylene fuel (flame temperatures are about 2400 K) used for the IDF create an appropriate environment for flame flicker. To investigate the possibility that the IDF oscillates naturally, unsteady calculations were performed for the same flow conditions using all three chemical-kinetics mechanisms. Surprisingly, the unsteady simulations resulted in a flame with large vortices forming outside the flame surface. Stably oscillating unsteady flames were obtained within 10,000 time steps of the calculations. Instantaneous temperature fields of the unsteady IDF that were simulated using the three mechanisms are shown in the right halves of Figs. 5a–5c.

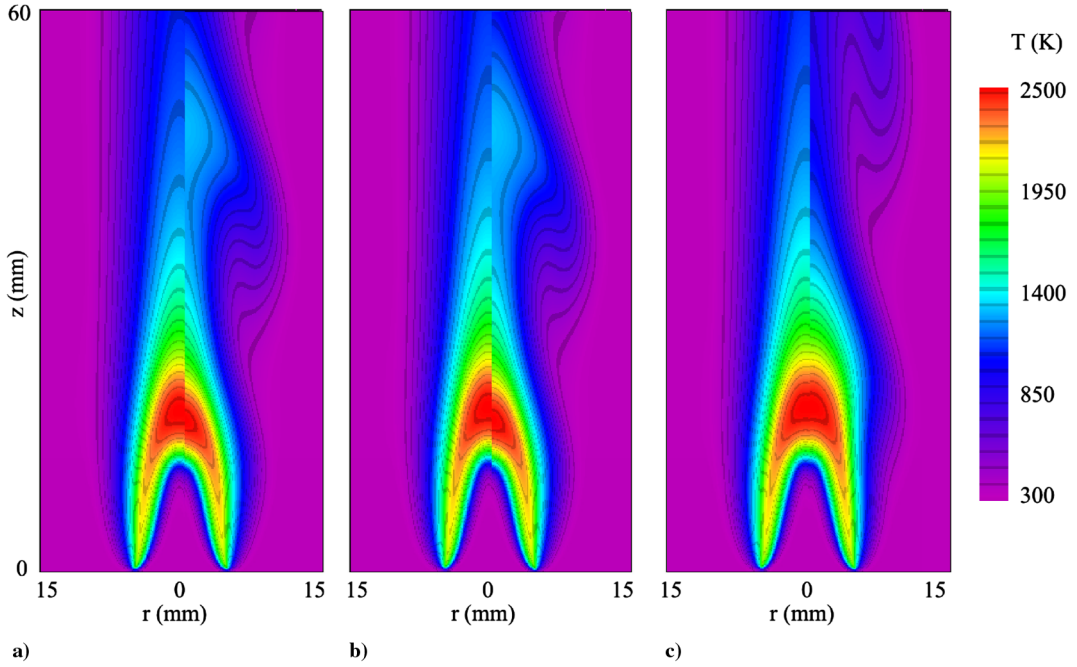

Fig. 5 Steady-state (left) and unsteady (right) ethylene–air, inverse nonpremixed flames simulated using a) Wang–Frenklach, b) NIST, and c) enhanced NIST mechanisms. Temperature distributions are shown.

Whereas the phases of the flames in Figs. 5a and 5b are matched, the phase of the flame in 5c is selected such that it is 180 deg from the other two. The unsteady temperature field upstream of the flame tip ($0 < z < 18$ mm) plotted in Fig. 5c is similar to that of the steady-state flames shown in Figs. 5a–5c. However, the large vortical structure ~30 mm in length that formed in the downstream location distorted the temperature field of the unsteady flame. When this vortical structure moved closest to the burner surface ($z = 0$), it squeezed the high-temperature region and made the flame temporarily shorter in Figs. 5a and 5b than the steady-state flame. Calculation time for the unsteady simulation performed with the 366-species, 3698-reaction mechanism was ~128 s/time step, and the solution in Fig. 5c was plotted after 15 days of calculations.

Benzene concentrations predicted by the three ethylene–air combustion models (Wang–Frenklach, NIST, and comprehensive NIST) are shown in Figs. 6a–6c, respectively. Steady-state and unsteady solutions are shown on the left and right halves of these images, respectively. Although nearly identical temperatures are predicted by the Wang–Frenklach and the two NIST mechanisms (Fig. 5), the benzene concentrations predicted by these mechanisms are quite different. The Wang–Frenklach mechanism yielded only ~50% of benzene that was predicted by the two NIST mechanisms. Although peak benzene concentration in the steady-state flame was established near the flame tip ($z \sim 20$) in the Wang–Frenklach mechanism (left half of Fig. 6a), it was established near the flame base in the NIST mechanisms (left halves of Figs. 6b and 6c). Interestingly, the buoyant vortex formed outside the flame surface in the unsteady simulation (Fig. 6b) has increased the benzene concentration significantly near its leading edge ($z \sim 45$ in Fig. 6b). Obtaining near identical solutions (Figs. 5 and 6) with different-size chemical-kinetics mechanisms is as expected and demonstrates the accuracy of the UNICORN code in incorporating large chemical-kinetics mechanisms.

C. Studies on JP-8–Air Nonpremixed Jet Flames

Axisymmetric calculations were performed for the opposing-jet JP-8 flame (similar to that shown in Fig. 2) using the UNICORN code. Four detailed chemical-kinetics models, namely, Violi-small [5], Violi-large [5], Zhang [6], and Mawid [7], were used for representing JP-8–air combustion. The Violi-small mechanism consists of 161 reactions and 1538 reactions (some of them are lumped) [5] . The Violi-large mechanism consists of 216 species and 9654 reactions (some of them are also lumped). The Zhang mechanism [6] consists of 208 species and 2186 elementary reactions. The Mawid mechanism [7] consists of 226 species and 3230 elementary reactions. Whereas the first three mechanisms use their own surrogate mixtures for representing JP-8 fuel, the Mawid mechanism employs one of the three surrogate mixtures developed at AFRL/RZ [39]. The chemical compositions of these surrogate mixtures are given in Table 1. The physical domain between the two nozzles (14 mm in the axial direction and 20 mm in the radial direction) was represented using a 201×31 grid system, which resulted in a uniform grid spacing of 70 μm across the flame. The fuel/N_2 ratio used in the calculations was 0.08. Experiments for this flame were conducted by Holley et al. [40]. The temperatures of the fuel and oxidizer streams were set to the measured values of 394 and 294 K, respectively. Initially, a stable flame was established for a low-strain-rate case of 28.6 s^{-1}. The corresponding fuel and oxidizer velocities were 0.2 and 0.2 m/s, respectively. Calculations for this flame were repeated by gradually increasing the strain rate (velocities) until the flame along the centerline was extinguished. The entire procedure, starting from establishing an initial flame to obtaining an extinguished flame, was repeated with each chemical-kinetics mechanism and surrogate mixture.

The flame response to an increase in strain rate predicted by different chemical-kinetics models is shown in Fig. 7. Here, the peak temperature along the centerline ($r = 0$) is plotted at different strain rates. Because of chemical nonequilibrium, the temperature of the flame decreased with strain rate. Data from each chemical-kinetics-model calculation up to the extinction limit are shown in Fig. 7. The measured extinction limit of 150 s^{-1} is shown with a vertical box. The width of the box corresponds to the experimental uncertainty of 3.5% reported by Holley et al. [40]. Calculations with the Mawid mechanism [7] were made using three surrogate mixtures identified as surrogate 1, surrogate 2, and surrogate 3. JP-8 fuel represented in the Violi mechanisms [5] is identical to surrogate 1. Among the four chemical-kinetics models considered, the Violi mechanisms predicted extinction strain rate more accurately than the other two. The Violi-small and the Violi-large mechanisms yielded nearly the same relationship between peak temperature and strain rate. A small but gradual deviation in peak temperature at higher strain rates

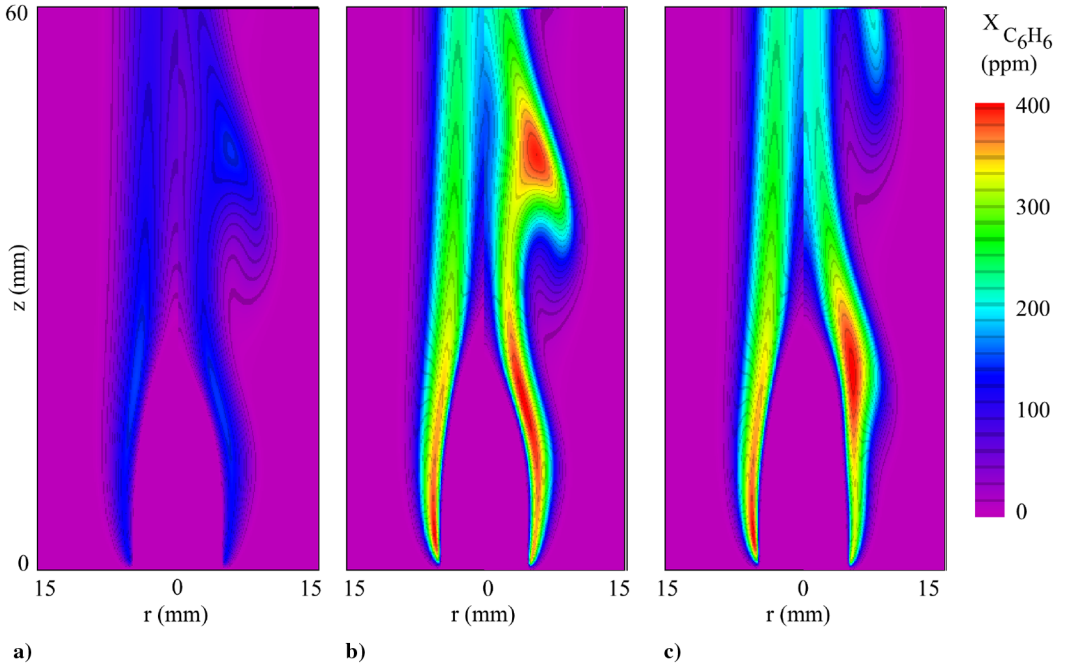

Fig. 6 Benzene concentrations in ethylene–air, inverse nonpremixed flames shown in Fig. 5. Calculations made with a) Wang–Frenklach, b) NIST, and c) enhanced NIST mechanisms.

Table 1 Representation of JP-8 fuel in various chemical-kinetics models

Fuel components	Violi-small mechanism [5]	Violi-large mechanism [5]	Zhang mechanism [6]	Mawid mechanism [7]		
				Surrogate 1	Surrogate 2	Surrogate 3
n-decane (*n*-C10H22)	0	0	0	16.2	0	25
n-dodecane (*n*-C12H26)	30	30	73.5	21	30	25
n-tetradecane (*n*-C14H30)	20	20	0	15.6	20	20
n-hexadecane (n-C16H34)	0	0	0	10.2	0	0
i-octane (I-C8H18)	10	10	5.5	5.7	10	5
Cyclooctane (*c*-C8H16)	0	0	0	4.7	0	0
Methylnaphthalene MCH (C11H10)	20	20	10	5.1	20	5
1-methylnaphthalene (C11H10)	0	0	0	3.9	0	0
Tetralin (C10H12)	5	5	0	4.1	5	0
1, 2, 4, 5-tetramethylbenzene (C9H12)	0	0	0	4.4	0	0
Butylbenzene (C10H14)	0	0	0	4.6	0	0
m-xylene (C8H10)	15	15	0	4.5	15	0
Toluene (C7H8)	0	0	10	0	0	20
Benzene (C6H6)	0	0	1	0	0	0
Molecular weight	**144.38**	**144.38**	**151.3**	**156.87**	**144.38**	**146.89**

predicted by these two mechanisms should be noted. The extinction strain rate of 136 s^{-1} predicted by these two mechanisms is within 90% of the measured value.

The elementary-reaction-based model developed by Zhang [6] yielded the most stubborn flame from an extinction point of view, even though the flame itself was not as strong (based on peak temperature) as the ones predicted by the semi-elementary-reaction-based mechanisms of Violi [5]. The importance of an accurate surrogate mixture for representing JP-8 fuel is evident from the calculations made with the Mawid mechanism [7]. The three surrogate mixtures yielded different temperature-strain-rate relationships (Fig. 7). Surrogate 1 yielded the lowest flame temperatures, which decreased further and rather rapidly with strain rate. Surrogates 2 and 3 yielded nearly the same extinction limits, with the latter mixture resulting in a slightly closer extinction limit when compared with the measured value. Interestingly, the flame temperature predicted with surrogate 2 was higher than that predicted with surrogate 3 when the strain rate was low, and lower when the stain rate was high. The major difference among the surrogate mixtures is that surrogate 1 contains additional parent compounds such as hexadecane (10.2%), cyclooctane (4.7%), methylnaphthalene (3.9%), tetramethylbenzene (4.4%), and butylbenzene (4.6%). A numerical experiment was conducted by systematically removing these compounds from surrogate 1. Calculations were repeated for the opposing-jet flame for different stretch rates; the results are shown in Fig. 8 and suggest that removal of hexadecane from the surrogate 1 mixture significantly increases the flame temperature (~108 K) and the extinction limit predicted by the Mawid mechanism.

Calculations for a JP-8 coaxial nonpremixed jet flame were performed using the four chemical-kinetics models. The simulated burner has a central fuel tube of 0.6 cm radius and is surrounded by a 5 cm radius coflowing air. A preheated fuel–N_2 mixture at 500 K and with 90% fuel by mass was issued at a velocity of 2 cm/s. The coannular flow consisted of room-temperature air and was issued at a velocity of 5 cm/s. A computational grid of 151 × 61 was used for discretizing the physical domain of 10 × 5 cm in axial and radial directions. Grid clustering was used for placing most of the grid points in the flame zone. Initial conditions (flame) for the detailed chemistry calculations were obtained from the simulation using a global-chemistry UNICORN code.

Results for the coaxial nonpremixed jet flame obtained with the Violi-small, Violi-large [5], and Zhang [6] models are shown in Figs. 9a–9c, respectively. Here, isocontours of methylcyclohexane (in dashes) and H_2 (in solid lines) are superimposed on the temperature distribution (in gray scale) on the left half of each figure. Isocontours of benzene (dashes), OH (solid lines), and temperature (in gray scale) are shown on the right halves.

In general, all three chemistry models predicted nearly the same flame shape, with the base region burning hotter than the tip region. Flames are slightly shifted from the inlet boundary as imposed by the stability criterion of the nonpremixed jet flames. However, several important differences exist in these predictions. The Violi-small and Violi-large mechanisms [5] resulted in nearly the same flames, except that the latter mechanism generated more H_2 and benzene inside the flame, and methylnaphthalene (MCH) was present in locations slightly farther downstream in the core region (Figs. 9a and 9b). The thermal layer (flame thickness) is wider for the Violi-large

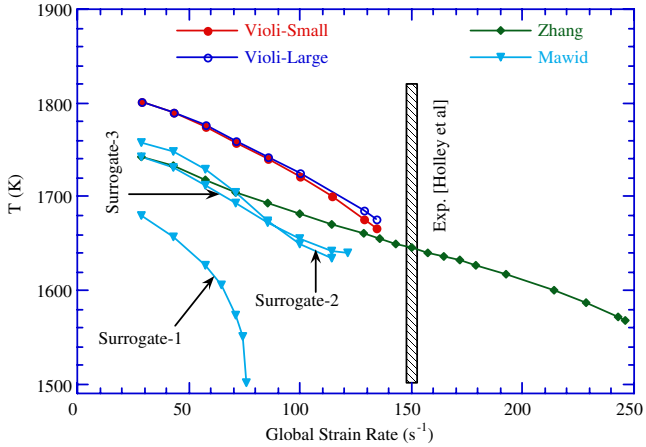

Fig. 7 Variations of peak temperature of nonpremixed, opposing-jet JP-8 flame with strain rate obtained using different chemical-kinetics mechanisms. Measured extinction strain rate is shown with vertical bar.

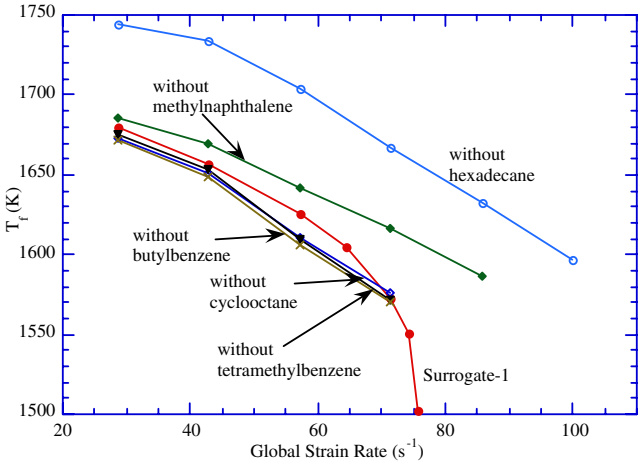

Fig. 8 Influence of parent compounds in surrogate 1 mixture of Mawid's [7] JP-8 mechanism on predicting flame extinction.

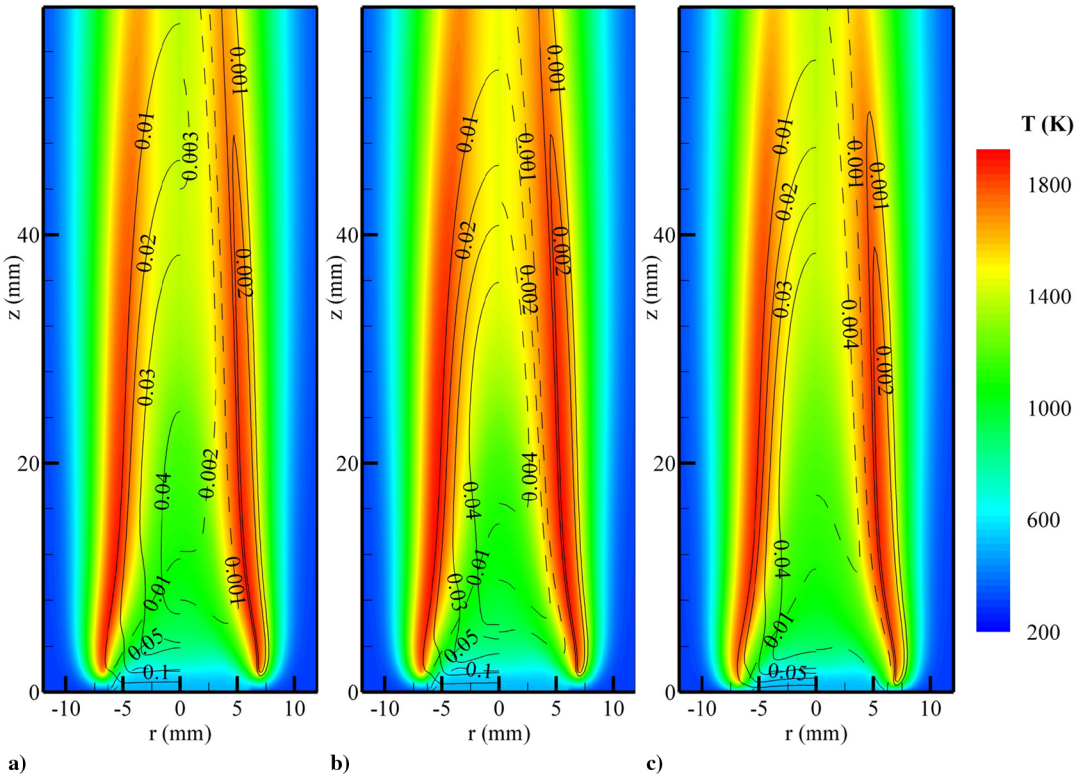

Fig. 9 Structure of JP-8 nonpremixed flame predicted using a) Violi-small, b) Violi-large, [5], and c) Zhang [6] mechanisms. Isocontours of MCH (dashed) and H_2 (solid) superimposed on temperature distribution on left half; isocontours of benzene (dashed) and OH (solid) superimposed on right half.

flame, which resulted in a hotter core region in Fig. 9b. As expected from the opposing-jet-flame calculations (Fig. 7), which suggested a much higher extinction strain rate for the Zhang mechanism [6], the coaxial nonpremixed flame predicted by this mechanism (Fig. 9c) is much closer to the inflow boundary than those predicted by the other models. Although there was 1% benzene in the surrogate mixture of the Zhang mechanism, it was all being consumed quickly in the core region and did not enhance the benzene produced in the flame region (Fig. 9c).

D. Studies on Effect of Di-Tertiary-Butyl-Peroxide on JP-8 Flames

Di-Tertiary-Butyl-Peroxide (DTBP) additive is known for improving the ignition characteristics of hydrocarbon fuels. It has

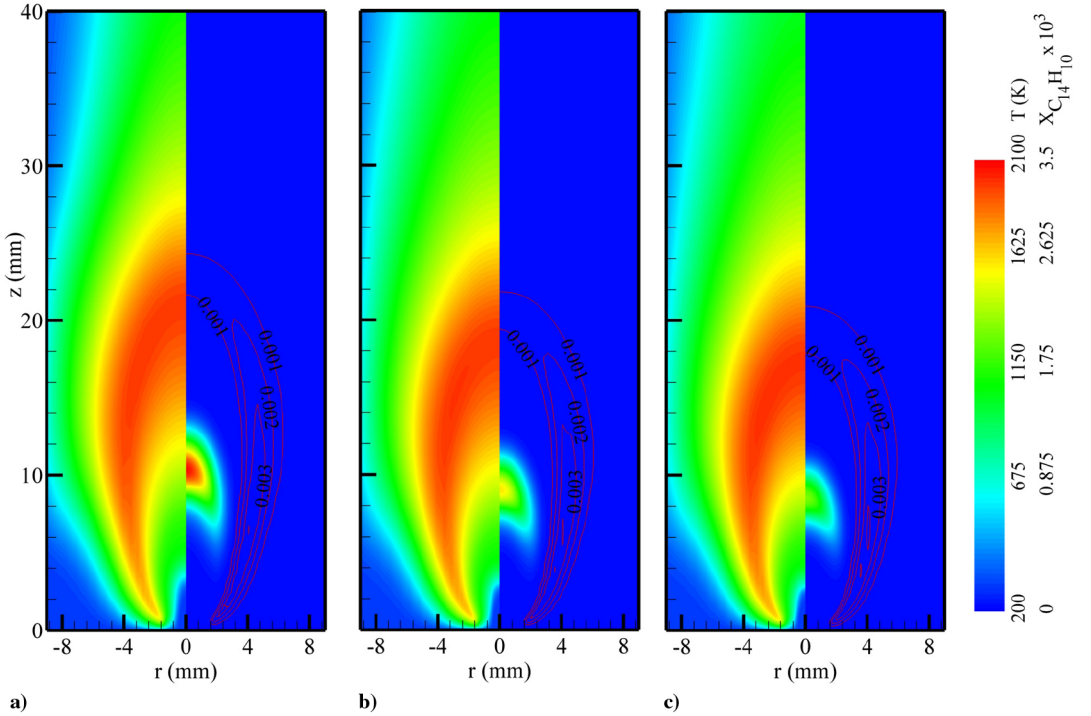

Fig. 10 Effect of DTBP additive on a) low-speed, nonpremixed jet flame, b) base flame, and c) flames with 10 and 15% additive added to fuel jet, respectively. Temperature distributions shown on left half of each flame; phenanthrene $C_{14}H_{10}$ (gray scale) and OH (contours) concentrations shown on right half.

been shown experimentally that the addition of DTBP alters gas-phase combustion [41] and, in some cases, soot production. Drop-tube [42] experimental results indicated that adding DTBP to fuel could reduce the amount of soot produced. For investigating the effects of DTBP on a JP-8 flame, a detailed chemical-kinetics model developed by Bozzelli [43], consisting of 98 species and 724 additional reactions, was added to the Zhang JP-8 mechanism [6]. The final Zhang–Bozzelli chemical-kinetics model derived for studying the effects of DTBP on JP-8 fuel has 306 species and 2910 reactions. The flame chosen for this study was a pure nonpremixed flame formed between gaseous JP-8 fuel and air. The velocity of the fuel, injected from a 1.0-mm-diam tube at room temperature, was 0.2 m/s. The annulus air velocity was 0.05 m/s. DTBP additive was added to the fuel jet by replacing an equal amount of JP-8, such that the exit velocity of the fuel jet was not altered. Axisymmetric calculations for this nonpremixed jet flame were performed for various concentrations of DTBP on a nonuniform grid system of 151×71.

Results obtained for the base flame (without addition of DTBP) are shown in Fig. 10a, and those for the flames with 10 and 15% DTBP added to the fuel jet are shown in Figs. 10b and 10c, respectively. Whereas gray-scale distributions of isotemperature are shown on the left halves of these figures, gray-scale distributions of phenanthrene ($C_{14}H_{10}$) are shown on the right halves. Distributions of the OH radical are superimposed in the right halves of the images. Phenanthrene was selected as a representative polycyclic-aromatic-hydrocarbon species that traces soot inception and growth. Figure 10a suggests that significant preheating of fuel before entering the flame zone is taking place. The flame, in general, is burning intensely in the tip region, with lower temperatures in the shoulder region. The peak temperature is about 2000 K. Fuel at room temperature exists for only a distance of ~5 mm in the fuel jet, at which location low-temperature ignition is taking place. Parent compounds of the JP-8 surrogate are decomposing into lower hydrocarbon fuels (such as C_2H_4, CH_4, and H_2) between this ignition location and the flame surface (peak-temperature location). Almost all of the phenanthrene produced in this flame is located upstream of the flame tip. Based on the phenanthrene distribution, it is expected that soot in this flame will develop along the axis of symmetry and in the neighborhood of the flame tip. The effects of DTBP on JP-8 fuel appear to be marginal. Addition of 10% DTBP reduced the flame size slightly (~2 mm in height), as shown in Fig. 10b. As expected, DTBP improved the ignition characteristics of the fuel. Note a decrease in the height of the room-temperature fuel jet and an increase in the OH concentration when 10% DTBP was added. Interestingly, phenanthrene concentration decreased by ~50%. These effects became more pronounced, as shown in Fig. 10c, when 15% DTBP was added to the fuel jet. To confirm this, further studies must be conducted using DTBP chemistry along with other JP-8 chemical kinetics (Violi-large [5], and Mawid [7]). The robust UNICORN code is capable of performing multidimensional calculations for a nonpremixed jet flame using these mechanisms.

V. Conclusions

The multidimensional CFD model UNICORN has been extensively validated in the past by simulating various steady and unsteady opposing- and coflowing-jet premixed and nonpremixed flames, and by comparing the results with experimental data [8], lending confidence in the accuracy of the simulations made using UNICORN for the structures of dynamic flames. To prepare for current and future demands for simulations of multidimensional flames established from commercial fuels, a robust and efficient UNICORN code that could handle large chemical-kinetics mechanisms with ease was developed. Following a software-generated CFD approach, a separate UNICORN code for a given chemical-kinetics mechanism was prepared. This approach virtually eliminated the human errors that occur when incorporating large chemical-kinetics mechanisms in a CFD code. The efficiency of the UNICORN code has been improved through the use of a submixture concept while evaluating transport properties and rapidly expanding grid systems. The robustness of the UNICORN code has been improved by making use of an implicit approach for solving species-conservation equations with large chemical source terms. Several sample simulations have been presented for demonstrating the abilities of the UNICORN code in handling very large chemical-kinetics mechanisms. Handling of stiffness, caused by the large source terms associated with combustion chemistry, has been demonstrated in the study on laminar-flamelet theory for stretched laminar nonpremixed flames where limits on flame thickness were examined through increasing the reaction rates by an order of magnitude. Efficiency of the calculations was demonstrated by conducting a parametric study on the role of parent compounds of a JP-8 surrogate mixture in predicting flame extinguishment. Retention of the accuracy of the UNICORN code while using very large chemical-kinetics mechanisms was demonstrated by simulating a naturally oscillating buoyant nonpremixed flame using models with 99 species, 1066 reactions; 225 species, 1634 reactions; and 366 species, 3698 reactions. Ease of incorporating large chemical-kinetics models was demonstrated in a study of additive effects on a JP-8 flame conducted by merging Zhang's JP-8 mechanism [6] with Bozzelli's Di-Tertiary-Butyl-Peroxide mechanism [43].

Acknowledgments

Financial support for this work was provided by the U.S. Air Force Office of Scientific Research (Julian Tishkoff), the Strategic Environmental Research and Development Program (Charles Pellerin), and U.S. Air Force Contract no. F33615-03-D-2329 (Tim Edwards and Vince Belovich). The authors thank Marian Whitaker for editorial help.

References

[1] Rogg, B., "RUN1DL: The Cambridge Universal Laminar Flamelet Computer Code," *Reduced Kinetic Mechanisms for Applications in Combustion Systems*, edited by N. Peters and B. Rogg, Lecture Notes in Physics m15, Springer–Verlag, Heidelberg, Germany, 1993, pp. 350–351.

[2] Lutz, A. E., Kee, R. J., Grcar, J. F., and Rupley, F. M., "OPPDIF: A Fortran Program for Computing Opposed Flow Diffusion Flames," Sandia National Lab. SAND96-8243, 1996.

[3] Kee, R. J., Miller, J. A., and Jefferson, T. H., "CHEMKIN: A General-Purpose, Problem-Independent, Transportable, Fortran, Chemical Kinetic Code Package," Sandia National Lab. TR SAND80-8003, 1980.

[4] Katta, V. R., Mawid, M., Sekar, B., Corporan, E., Zelina, J., Roquemore, W. M., and Montgomery, C. J., "Comparison of Chemical-Kinetics Models for JP-8 Fuel in Predicting Premixed and Nonpremixed Flames," *42nd AIAA/ASME/SAE/ASEE Joint Propulsion Conference and Exhibit*, AIAA Paper 2006-4745, July 2006.

[5] Violi, A., Yan, S., Eddings, E. G., Sarofim, A. F., Granata, S., Faravelli, T., and Ranzi, E., "Experimental Formulation and Kinetic Model for JP-8 Surrogate Mixtures," *Combustion Science and Technology*, Vol. 174, Nos. 1–12, 2002, pp. 399–417. doi:10.1080/00102200215080

[6] Zhang, H., Ph. D. Dissertation, Dept. of Chemical Engineering, Univ. of Utah, Salt Lake City, UT, May 2005.

[7] Mawid, M. A., and Sekar, B., "Detailed Chemical Kinetic Modeling of JP-8/Jet-A Ignition in High Pressure Shock Tube," *42nd AIAA/ASME/SAE/ASEE Joint Propulsion Conference and Exhibit*, AIAA Paper 2006-5102, July 2006.

[8] Roquemore, W. M., and Katta, V. R., "Role of Flow Visualization in the Development of UNICORN," *Journal of Visualization*, Vol. 2, Nos. 3–4, 2000, pp. 257–272.

[9] Briones, A. M., Aggarwal, S. K., and Katta, V. R., "Numerical Investigation of Flame Liftoff, Stabilization, and Blowout," *Physics of Fluids*, Vol. 18, No. 4, 2006, p. 043603. doi:10.1063/1.2191851

[10] Anna, A. D., Kent, J. H., and Santoro, R. J., "Investigation of Species Concentration and Soot Formation in a Co-Flowing Diffusion Flame of Ethylene," *Combustion Science and Technology*, Vol. 179, Nos. 1–2, 2007, pp. 355–369. doi:10.1080/00102200600812419

[11] Liu, F., Guo, H., Smallwood, G. J., and Gulder, O. L., "Numerical Modeling of Soot Formation and Oxidation in Laminar Coflow Non-Smoking and Smoking Ethylene Diffusion Flame," *Combustion Theory and Modeling*, Vol. 7, No. 2, 2003, pp. 301–315. doi:10.1088/1364-7830/7/2/305

[12] Mizobuchi, Y., Shinjo, J., Ogawa, S., and Takeno, T., "Numerical Study on the Formation of Diffusion Flame Islands in a Turbulent Hydrogen Jet Lifted Flame," *Proceedings of the Combustion Institute*, Vol. 30, No. 1, 2005, pp. 611–619. doi:10.1016/j.proci.2004.08.142

[13] Kaplan, C. R., and Kailasanath, K., "Flow-Field Effects on Soot Formation in Normal and Inverse Methane-Air Diffusion Flames," *Combustion and Flame*, Vol. 124, Nos. 1–2, 2001, pp. 275–294. doi:10.1016/S0010-2180(00)00196-6

[14] Bennett, B. A. V., Mcenally, C. S., Pfefferle, L. D., and Smooke, M., "Computational and Experimental Study of Axisymmetric Coflow Partially Premixed Ethylene/Air Flames," *Combustion and Flame*, Vol. 127, Nos. 1–2, 2001, pp. 2004–2022. doi:10.1016/S0010-2180(01)00306-6

[15] Haworth, D. C., Cuenot, B., and Poinsot, T., "Direct Numerical Simulation and Modeling for Lean Stratified Propane-Air Flames," *Combustion and Flame*, Vol. 128, Nos. 1–2, 2002, pp. 1–21. doi:10.1016/S0010-2180(01)00328-5

[16] Maroteaux, F., Noel, L., and Ahmed, A., "Numerical Investigations on Methods to Control the Rate of Heat Release of HCCI Combustion Using Reduced N-Heptane with Multidimensional CFD Code," *Combustion Theory and Modeling*, Vol. 11, No. 4, 2007, pp. 501–525. doi:10.1080/13647830600952891

[17] Ebrahimi, H., and Malo-Molina, F., "Numerical Investigation of 2-D and 3-D Multitube Pulse Detonation Using H2 and JP8 Fuel," *42nd AIAA Aerospace Sciences Meeting and Exhibit*, AIAA Paper 2004-0465, Jan. 2004.

[18] Katta, V. R., Goss, L. P., and Roquemore, W. M., "Numerical Investigations of Transitional H_2/N_2 Jet Diffusion Flames," *AIAA Journal*, Vol. 32, No. 1, 1994, p. 84.

[19] Wilke, C. R., "Viscosity Equation for Gas Mixtures," *Journal of Chemical Physics*, Vol. 18, No. 4, April 1950, pp. 517–519. doi:10.1063/1.1747673

[20] Hirschfelder, J. O., Curtiss, C. F., and Bird, R. B., *Molecular Theory of Gases and Liquids*, Wiley, New York, 1954.

[21] Williams, F. A., *Combustion Theory*, Perseus, Reading, MA, 1985.

[22] Leonard, B. P., "Stable and Accurate Convective Modeling Procedure Based on Quadratic Upstream Interpolation," *Computational Methods in Applied Mechanical Engineering*, Vol. 19, 1979, p. 59.

[23] Katta, V. R., and Roquemore, W. M., "Numerical Studies on Trapped-Vortex Concepts for Stable Combustion," *Transactions of the ASME: Journal of Engineering for Gas Turbines and Power*, Vol. 120, April 1998, p. 60. doi:10.1115/1.2818088

[24] Katta, V. R., Goss, L. P., and Roquemore, W. M., "Simulation of Vortical Structures in a Jet Diffusion Flame," *International Journal of Numerical Methods for Heat and Fluid Flow*, Vol. 4, No. 5, 1994, p. 413. doi:10.1108/EUM0000000004046

[25] Liang, L., Kong, S-C., Jung, C., and Reitz, R. D., "Development of Semi-Empirical Solver for Detailed Chemistry In Internal Combustion Engine Simulations," *Journal of Engineering for Gas Turbines and Power*, Vol. 129, No. 1, 2007, pp. 271–278. doi:10.1115/1.2204979

[26] Smooke, M. D., "Numerical Modeling of Laminar Diffusion Flames," edited by E. S. Oran and J. P. Boris, Vol. 135, Progress in Astronautics and Aeronautics, AIAA, Washington, D.C., 1991, pp. 183–223.

[27] Ito, T., Hosaka, T., Senda, J., and Fujimoto, H., "Numerical Investigation of Soot Formation in Diesel Jet Flame Using Detailed Kinetic Model," *Transactions of the Japan Society of Mechanical Engineers, Series B*, Vol. 71, No. 701, 2005, pp. 288–294.

[28] Hilbert, R., and Thevenin, D., "Autoignition of Turbulent Non-Premixed Flames Investigated Using Direct Numerical Simulations," *Combustion and Flame*, Vol. 128, Nos. 1–2, 2002, pp. 22–37. doi:10.1016/S0010-2180(01)00330-3

[29] Yoshida, K., and Takagi, T., "Transient Local Extinction and Reignition Behavior of Diffusion Flames Affected by Flame Curvature and Preferential Diffusion," *Proceedings of the Combustion Institute*, Vol. 27, 1998, pp. 685–692.

[30] Katta, V. R., Blevins, L. G., and Roquemore, W. M., "Dynamics of an Inverse Diffusion Flame and Its Role in Polycyclic-Aromatic-Hydrocarbon and Soot Formation," *Combustion and Flame*, Vol. 142, Nos. 1–2, 2005, pp. 33–51. doi:10.1016/j.combustflame.2005.02.006

[31] Katta, V. R., and Roquemore, W. M., "Simulation of Unsteady Flows in an Axisymmetric Research Combustor Using Detailed-Chemical Kinetics," *34th AIAA/ASME/SAE/ASEE Joint Propulsion Conference and Exhibit*, AIAA Paper 98-3766, July 1998.

[32] Katta, V. R., Takahashi, F., and Linteris, G. T., "Fire-Suppression Characteristics of CF_3H in a Cup Burner," *Combustion and Flame*, Vol. 144, No. 4, 2006, pp. 645–661. doi:10.1016/j.combustflame.2005.09.006

[33] Katta, V. R., and Roquemore, W. M., "Effect of Nitromethane on Soot Formation in Heptane Jet Diffusion Flame," *Fourth Joint Combustion Meeting of the U. S. Sections of the Combustion Institute*, Combustion Inst. Paper 198, March 2005.

[34] Peters, N., "Laminar Flamelet Concepts in Turbulent Combustion," *Proceedings of the Combustion Institute*, Vol. 21, 1986, pp. 1231–1256.

[35] Bilger, R. W., "The structure of turbulent nonpremixed flames," *Proceedings of the Combustion Institute*, Vol. 22, 1988, pp. 475–488.

[36] Wang, H., and Frenklach, M., "Detailed Kinetic Modeling Study of Aromatics Formation in Laminar Premixed Acetylene and Ethylene Flames," *Combustion and Flame*, Vol. 110, No. 1, 1997, p. 173. doi:10.1016/S0010-2180(97)00068-0

[37] Tsang, W., "Progress in the Development of Combustion Kinetics Databases for Liquid Fuels," *Data Science Journal*, Vol. 3, Jan. 2004, pp. 1–9. doi:10.2481/dsj.3.1

[38] Blevins, L. G., Fletcher, R. A., Benner, B. A., Steel, E. B., and Mulholland, G. W., "Existence of Young Soot in the Exhaust of Inverse Diffusion Flames," *Proceedings of the Combustion Institute*, Vol. 29, No. 2, 2002, pp. 2325–2333. doi:10.1016/S1540-7489(02)80283-8

[39] Schulz, W., "Oxidation Products of a Surrogate JP-8 Fuel," *ACS Petroleum Chemistry Division Preprints*, Vol. 37, No. 2, 1991, pp. 383–392.

[40] Holley, A. T., Dong, Y., Andac, M. G., and Egolfopoulos, F. N., "Ignition and Extinction of Non-Premixed Flames of Single-Component Liquid Hydrocarbons, Jet Fuels, and Surrogates," *Proceedings of the Combustion Institute*, Vol. 31, No. 1, 2007, pp. 1205–1213. doi:10.1016/j.proci.2006.07.208

[41] Mack, J. H., Dibble, R. W., Buchholz, B. A., and Flowers, D. L., "Effect of the Di-Tertiary Butyl Peroxide (DTBP) Additive on HCCI Combustion of Fuel Blends of Ethanol and Diethyl Ether," Society of Automation Engineers TP 2005-01-2135, 2005.

[42] Kobayashi, H., Howard, J. B., and Sarofim, A. F., "Coal Devolatilization at High Temperatures," *Proceedings of the Combustion Institute*, Vol. 16, 1976, pp. 411–425.

[43] Montgomery, C., Sarofim, A., Preciado, I., Marsh, N., Eddings, E., and Bozzelli, J., "Experimental and Numerical Investigation of Soot-Reducing Fuel Additives," *41st AIAA/ASME/SAE/ASEE Joint Propulsion Conference and Exhibit*, AIAA Paper 2005-4472, July 2005.

C. Kaplan
Associate Editor